

Initial Evaluation of the SAGE III/ISS Water Vapor Retrieval

David Huber¹, Robert Damadeo², Larry Thomason², David Flittner², Robert Manion¹,

Susan Kizer¹, James Moore¹, Scott Porter¹

¹Science Systems and Applications, Inc.

²NASA Langley Research Center



Introduction

The Stratospheric Aerosol and Gas Experiment operating on the International Space Station (SAGE III/ISS) is an occultation instrument that retrieves aerosol extinction and ozone, water vapor, and other trace gas concentrations. Water vapor in the stratosphere plays a significant role in ozone depletion and global temperature regulation making it an important species to monitor. The new SAGE III/ISS instrument provides high quality, vertically resolved profiles of water vapor throughout the stratosphere and upper troposphere. A discussion is presented on the sensitivity of the SAGE III/ISS water vapor product and provide an early evaluation of the retrieved profiles.

Methodology

The retrieval is performed from 60km to opaque cloud top in the spectral range of the water vapor $\rho\sigma\tau$ and one of the ozone Wulf absorption bands. It relies on 29 channel measurements at 869nm, 920nm, and 936 to 955nm at approximately 1nm spacing. The retrieval itself is performed by

1. smoothing 0.5km-binned transmission to a 1km vertical grid with 1-2-1 kernel;
2. removing the molecular scattering component to slant path absorption following Bucholz (1996);
3. solving simultaneously for H₂O, O₃, and aerosol extinction at 1km intervals:
 - a. H₂O slant path absorption modeled utilizing the Curtis-Godson Approximation,
 - b. O₃ slant path absorption fit using absorption cross-section data (Bogumil et al., 2003), and
 - c. aerosol slant path extinction resolved assuming a linear function of wavelength; and
4. interpolating retrieved water vapor to a 0.5km vertical grid.

Challenges

Weak Signal The water vapor and ozone signals are relatively weak in the $\rho\sigma\tau$ and Wulf bands, each comprising ~10% of the signal at peak wavelengths at 20km. In addition, the shape of the Wulf band feature is similar to one of the water vapor features, as shown in Figure 1, requiring an accurately shaped ozone cross-section for the retrieval.

Spectroscopy Modeling the water vapor features, in particular, necessitates a thorough understanding of the instrument's spectral sampling. For version 5.1, a rigorous method was developed to perform wavelength and band pass registration (see poster A31L-3094). Figure 2 shows the modeled and observed optical depth before and after applying this new method.

Etalon A hardware change for the SAGE III/ISS instrument prevented the attenuator plate etalon observed during the SAGE III/M3M mission. The etalon resulted in the appearance of a non-physical, altitude and wavelength dependent feature, as shown in Figure 3a between 90 and 100km. However, the SAGE III/ISS instrument is subject to additional sources of random noise, as evinced by Figure 3b, due in part to mechanical disturbances.

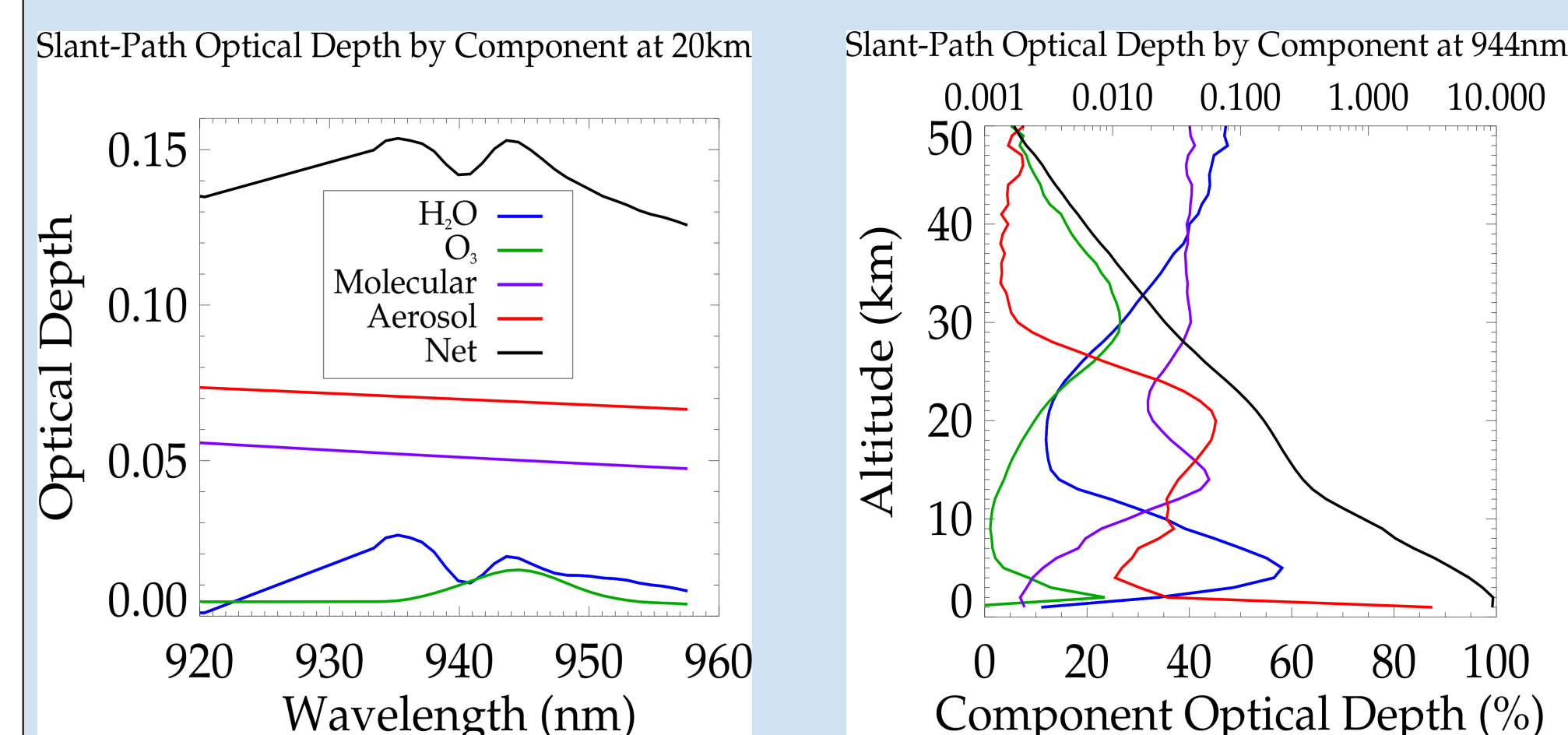


Figure 1. Median extinction components in the vicinity of the $\rho\sigma\tau$ band (left) at 20km and (right) as a function of altitude at the ozone Wulf band peak (944.5nm) for June 2018 between 30° and 50°N as modeled by the retrieval algorithm.

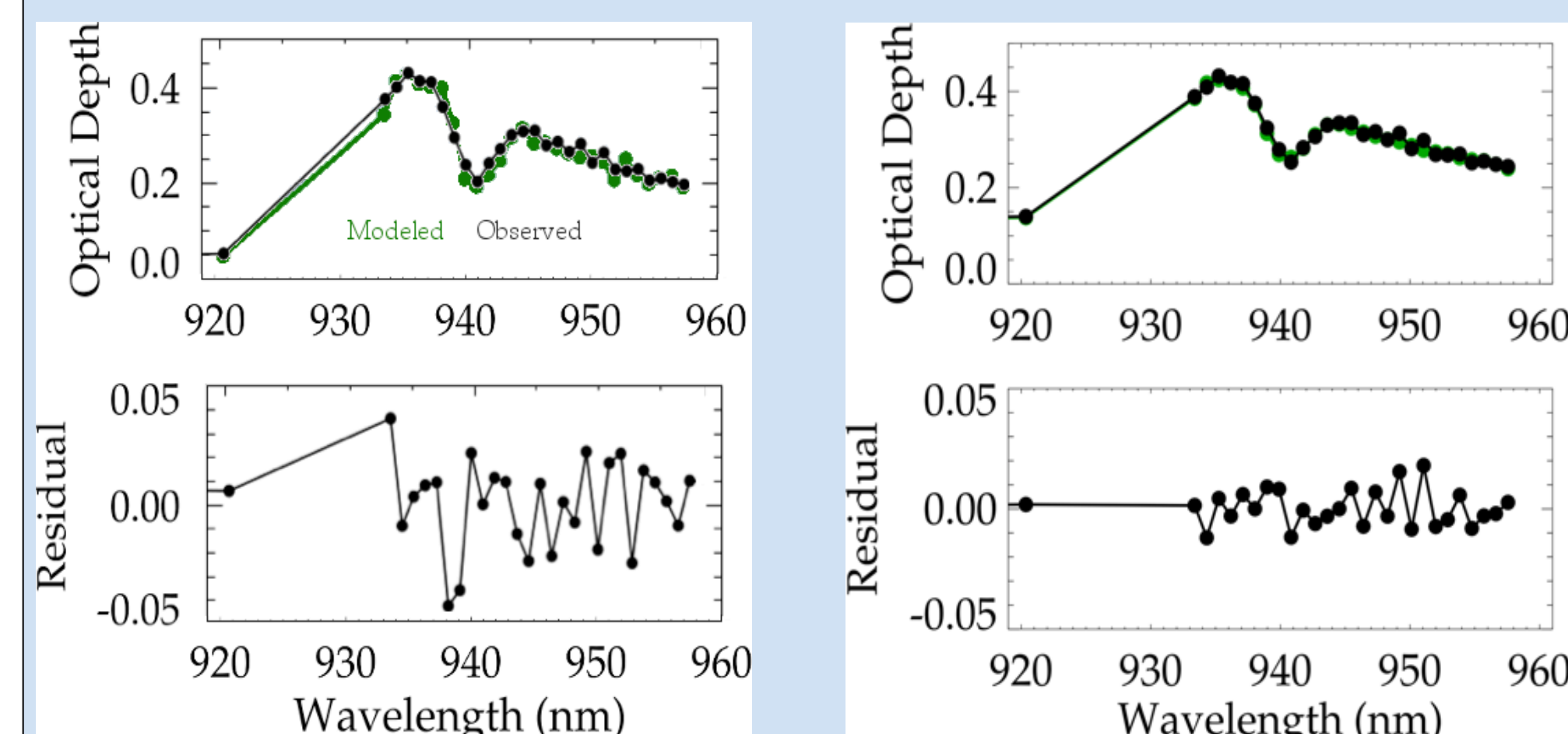


Figure 2. Median modeled and observed optical depth with the molecular scattering component of absorption removed using the (top left) version 5.0 and (top right) 5.1 retrieval algorithms and the residuals (bottom left and bottom right, respectively). Includes measurements from July 2017 where 50ppm < χ < 100ppm.

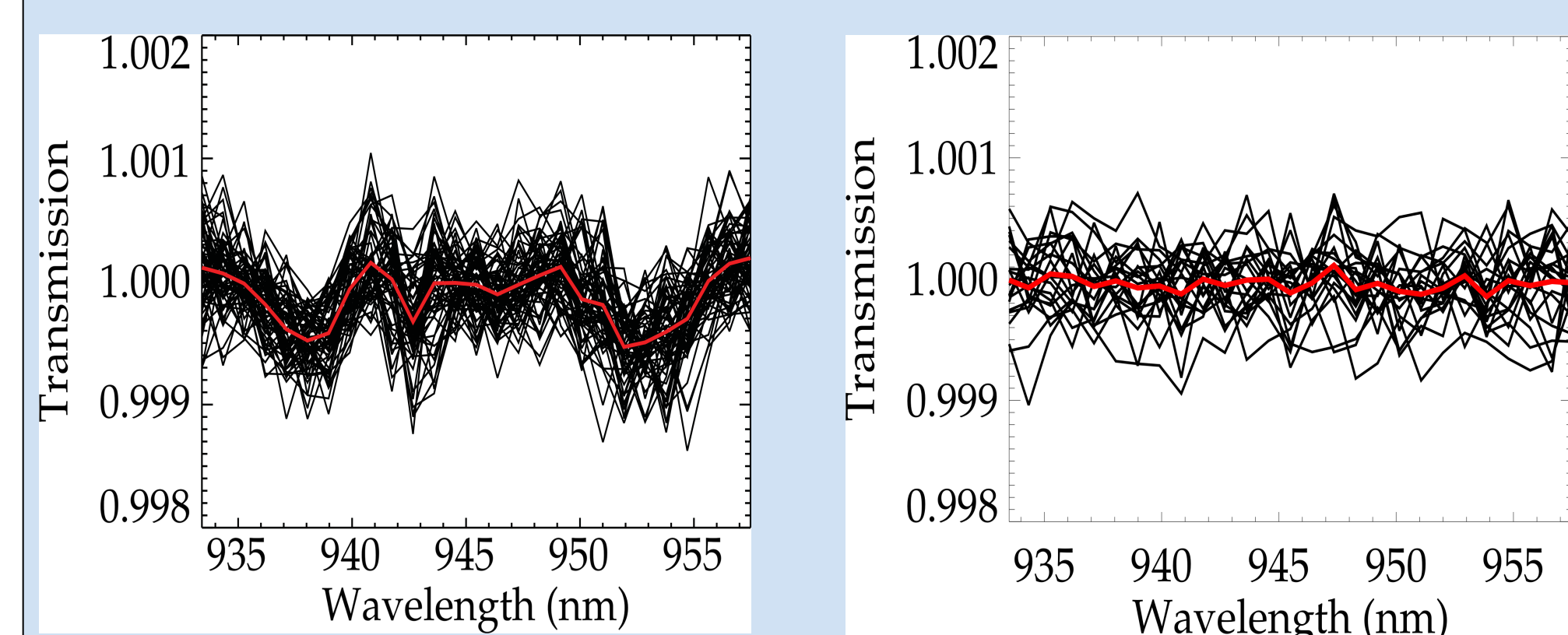


Figure 3. (Left) transmission from a SAGE III/M3M (Thomason et al., 2010) and SAGE III/ISS (right) event between 90 and 100km (black) and the average transmission (red).

Results

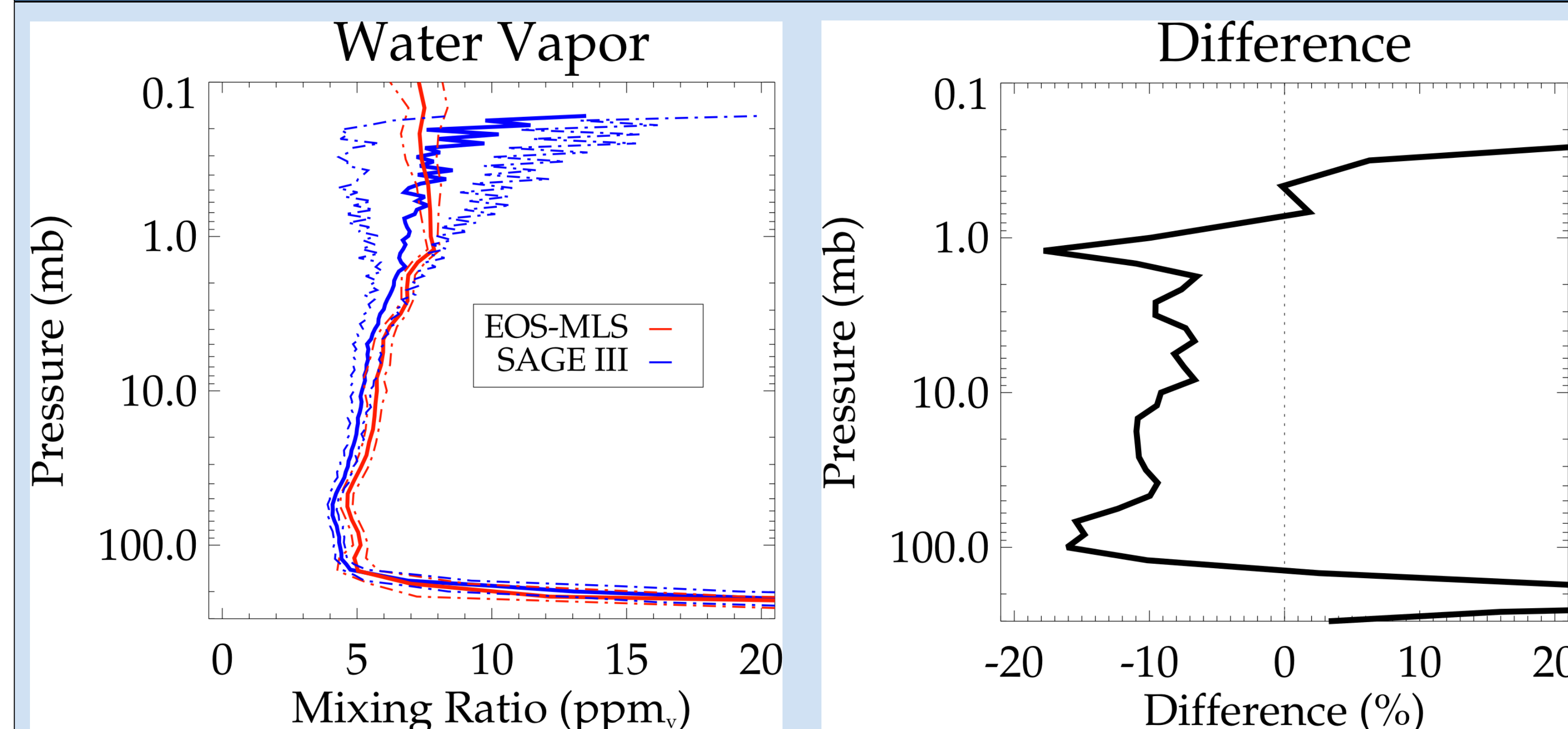


Figure 4. (Left) median SAGE III (blue) and EOS-MLS (red) water vapor mixing ratios and 25th and 75th percentiles (dot-dashed) for 331 coincident events between 30° and 50°N in November, 2017 and (right) difference between the medians.

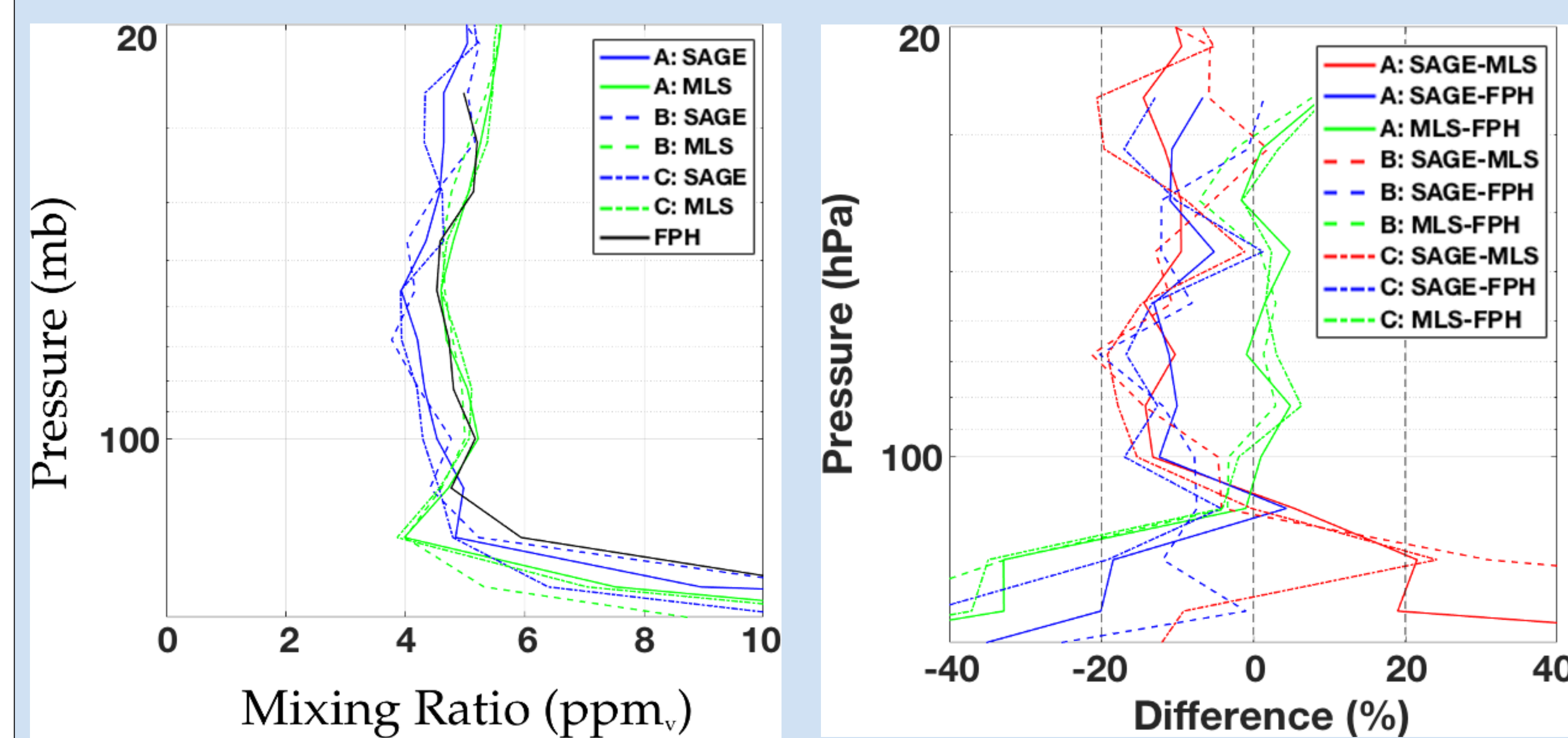


Figure 5. (Left) water vapor mixing ratio profiles for three coincident SAGE III (blue) and EOS-MLS (green) events as well as a frost point hygrometer (FPH) balloon sonde launched from Boulder, CO on 14 November 2017 and (right) their respective differences.

Measurement	Time (UTC)	Latitude (°N)	Longitude (°W)
A: SAGE	1401	41.7	107.0
A: MLS	0924	44.4	107.1
B: SAGE	1444	39.5	118.8
B: MLS	2114	38.5	119.0
C: SAGE	1311	39.7	95.5
C: MLS	0830	40.0	94.7
FPH	1720	40.0	105.2

Table 1. Measurement times and locations for the SAGE III and EOS-MLS measurements coincident with the balloon sonde measurement (FPH).

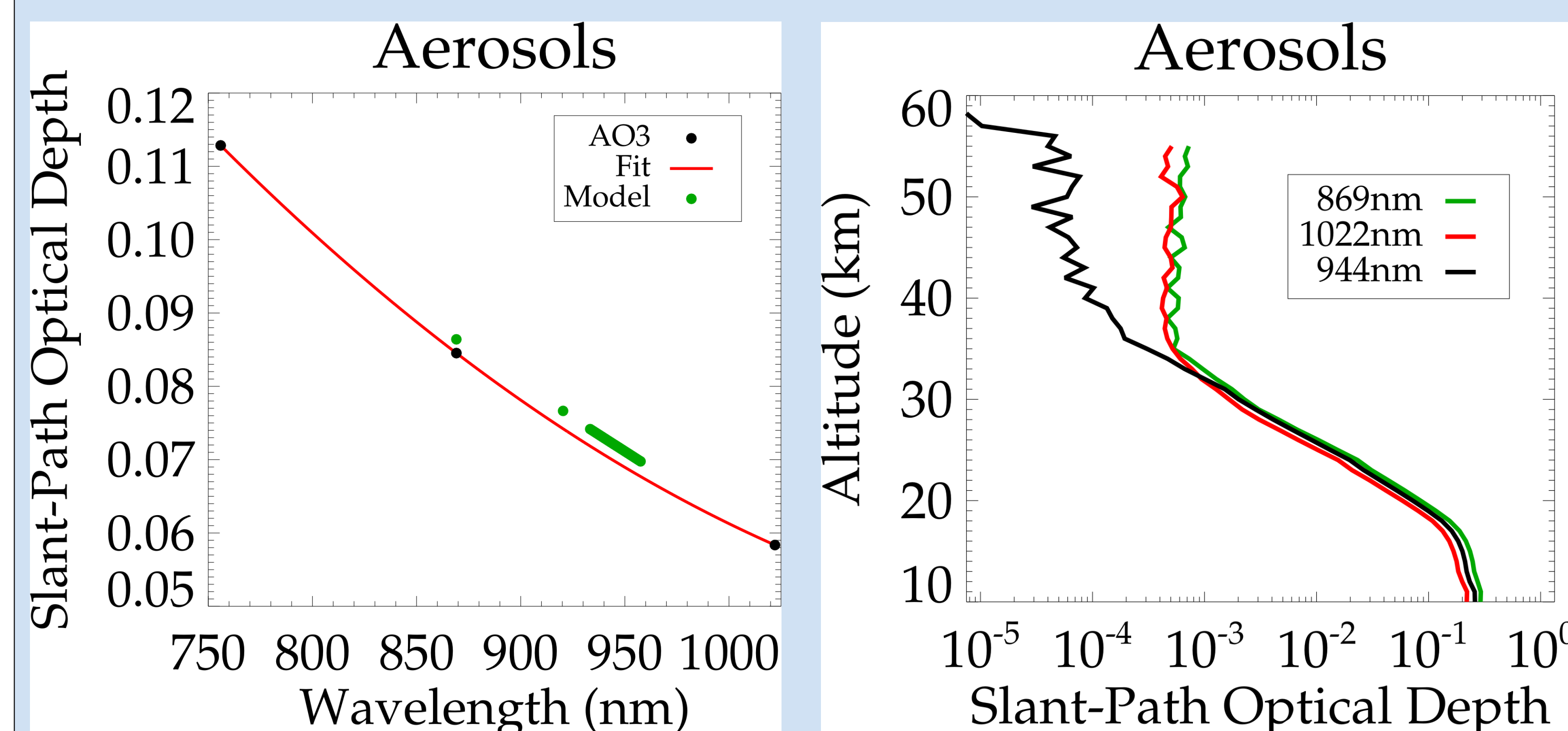


Figure 6. (Left) median aerosol slant-path optical depth as retrieved by the SAGE II-like algorithm at 756, 869, and 1022nm (AO3; black dots), a quadratic fit to the three points (Fit; red line), and median modeled slant-path optical depth from the water vapor retrieval (green dots) at 20km for the same 331 events as described in Figure 4. (Right) median aerosol slant-path optical depth profiles as retrieved by the SAGE II-like algorithm at 869 (green) and 1022nm (red) as well as the modeled slant-path optical depth from the water vapor retrieval at 944nm (black).

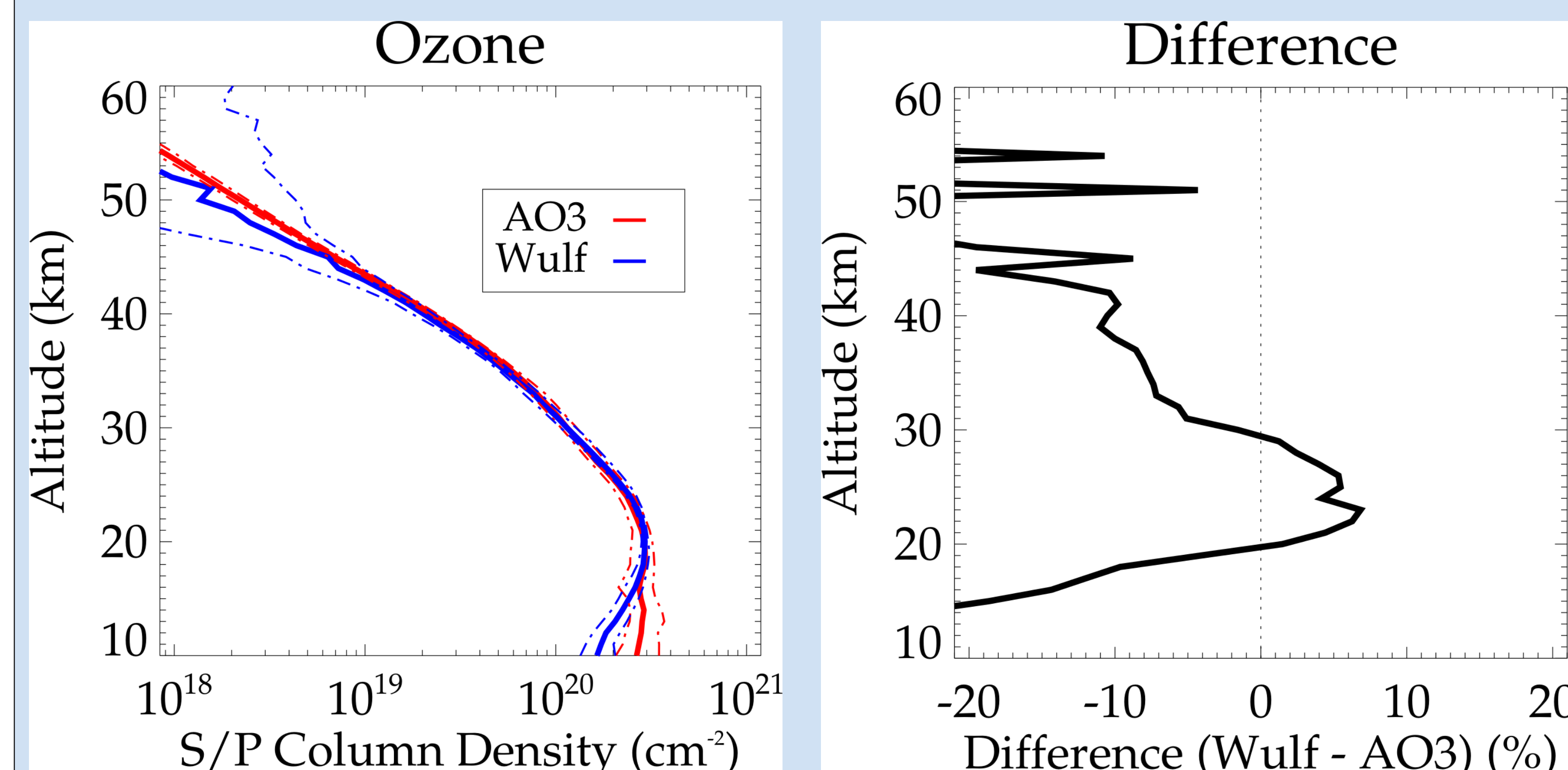


Figure 7. (Left) median ozone slant-path column density as retrieved by the SAGE II-like algorithm (AO3; red) and the water vapor retrieval (blue) and the 25th and 75th percentile for each (dot-dashed) from the 331 events described in Figure 4. (Right) the difference between the median profiles (Wulf - AO3).

Discussion

When comparing the retrieved quantities from the water vapor retrieval, it is evident that

1. the shape of the water vapor profiles in Figures 4 and 5 correlate well with EOS-MLS and balloon sonde FPH measurements, with an approximate 10% dry bias through most of the stratosphere compared with EOS-MLS,
2. towards the upper stratosphere, the water vapor profiles become quite noisy and wet-biased, as indicated in Figure 4,
3. retrieved aerosol extinction SPOD as shown in Figure 6 are biased high when compared with the AO3 retrieved aerosols,
4. the retrieved ozone slant-path column densities shown in Figure 7 are biased high near the peak and biased low elsewhere.

From this, we ascertain that

1. it may be that the high-biased aerosols contribute to the dry-biased water vapor retrieval,
2. the linear shape used for the aerosols in this band may not be the best choice,
3. the retrieved water vapor is unaffected by the relative magnitude of the ozone cross-sections in the Wulf-band compared tot the Chappuis and depends more upon the relative shape of those cross-section within the Wulf-band itself, and
4. the aerosol component of the retrieval plays a significant role in the determination of water vapor and it appears that the noise floor occure above ~45km in this spectral range such that the water vapor product is expected to be noisier above this altitude.

Future work

Transmission Product Improvements A thorough review of the transmission algorithm is ongoing and improvements made along the way will certainly benefit the water vapor product. In addition, the incorporation of data from the disturbance monitoring package (DMP) is expected to improve pointing knowledge, and thus transmission accuracy and precision (see poster A31L-3083).

Improve Handling Measurement Noise Noise in the water vapor channels may be handled better by co-adding pixels and/or performing a global fit retrieval. Of course, the improvements to the transmission product will determine the level of effort required to improve noise handling.

Improve Aerosol/Ozone Handling Over the coming months, we will be experimenting with new and better ways to resolve and/or clear ozone and aerosols. For ozone, this may include constraining the solution to the AO3 retrieval while for aerosols, clearing the low frequency component from transmission may yield better results. Tests will be performed to determine the optimal solutions for both.

References

- K. Bogumil, et al.: Measurements of molecular absorption spectra with the SCIAMACHY pre-flight model: instrument characterization and reference data for atmospheric remote sensing in the 230–2380 nm region, J. Photochem. Photobiol. A, 157–167 (2003).
- A. Bucholtz: Rayleigh-scattering calculations for the terrestrial atmosphere. Appl. Opt. **34**, 2765-2773 (1995).
- R. Manion, D. Flittner, J. Moore, C. Hill, K. Leavor: Wavelength Calibration for the SAGE III/ISS Instrument. AGU Fall Meeting, December 2018, Washington, DC. Poster Presentation A31L-3094.
- D. Marquardt: An algorithm for least-squares estimation of nonlinear parameters. J. Soc. Indust. Appl. Math. **11**, 431-441 (1963).
- A. Rowell, C. Hill, K. Leavor, D. Huber: Relative Pointing Correction Using the SAGE III ISS Disturbance Monitoring Package. AGU Fall Meeting, December 2018, Washington, DC. Poster Presentation A31L-3083.
- L. Thomason, J. Moore, M. Pitts, J. Zawodny, E. Chiou: An evaluation of the SAGE III version 4 aerosol extinction coefficient and water vapor data products. Atmos. Chem. Phys., **10**, 2159-2173 (2010).

Acknowledgement

SAGE III/ISS is a NASA Langley managed mission funded by the NASA Science Mission Directorate within the Earth Systematic Mission Program. Enabling partners are the NASA Human Exploration and Operations Mission Directorate, International Space Station Program and the European Space Agency. SSAI personnel are supported through the STARSS III contract NNL16AA05C.